Compliant Control of Threaded Fastener Insertion *

Edward J. Nicolson and Ronald S. Fearing
Department of EE&CS
University of California
Berkeley, CA 94720

Abstract

Controlled compliance and accommodation matrix techniques are considered for robust insertion of threaded fasteners. Errors in translational positioning are shown to be easily corrected. Errors in the angle of tilt between the threaded parts are shown to be much more difficult to correct and constrain the region of convergence for simple linear techniques.

1 Introduction

According to a study by Nevins and Whitney [Nevins 80] the insertion and tightening of threaded fasteners is one of the twelve most common assembly tasks, yet little published work has considered the type of control best suited for the assembly of threaded parts. This is surprising since threaded fasteners are unlikely to be eliminated from assembly operations due to their ability to be reassembled many times and to develop a variable preload, or force of assembly.

In robotics literature screw threading is often referred to as a typical task, yet, unlike the smooth peg-in-hole problem, a robust control solution for inserting threaded fasteners has not been presented. Recently [Tsujimura 91] presented a system identification technique to improve position control of screw threading. Their efforts were hampered by an imprecise robot and lack of a model for the threaded parts. [Tao 90] used a Remote Center of Compliance (RCC) technique, motivated by [Nevins 80, Whitney 82], but again without a model for the threaded parts. Regions of convergence were not presented.

[Blaer 62] provides guidelines for the rotational speed of a nut being fitted on to a bolt with a given axial stiffness when there are no orientation errors. When errors are allowed only for the position along the axis of the bolt, the control problem for this restricted case is one dimensional. The main result showed that

if the bolt rotates too fast for a given axial spring constant and position for the spring equilibrium point, then the nut will not begin to thread.

[Smith 80] provides a good overview of automatic screwdriver technology, unfortunately it is now ten years old. The most interesting method described requires monitoring of the torque and angle about the axis of rotation as the bolt is inserted. The plot of torque versus angle, called the "fastening signature," is compared against signatures for proper and failed assemblies to determine if the insertion proceeded correctly. In this manner Smith claims the ability to discriminate proper fastening from thread stripping and thread crossing as well as detecting faulty fasteners. According to [Weber] torque and angle monitoring is now the standard for high performance screw insertion. The data from these sensors is commonly used for statistical analysis of failure rates by process control engineers.

Current automatic insertion methods do not guarantee successful insertion. Hence bolts are often started by hand and then tightened with a machine. Manual threading uses heuristics to ensure proper assembly such as rotating the fastener the wrong way for half a turn and then rotating in the correct direction.

There are two obstacles to the full automation of screw threading: 1) feeding and holding the parts and 2) controlling the parts to ensure proper mating and detect part failures in the presence of positional uncertainty. Given current screw head geometries, the first problem is considerable. [Mikels 91] has addressed it by developing a helical head driver with a centering recess. The Torx^{TM} head is alone among current screwdriver heads in providing control of the bolt during insertion. For our experiments we drilled a hole in the center of the bolt and attached it to the motor directly to concentrate on the second problem, controlling the trajectory of the nut and bolt.

We proceed by reviewing the fundamentals of our screw model presented in [Nicolson and Fearing 91] in section 2. In section 3 we discuss the maximum tilt
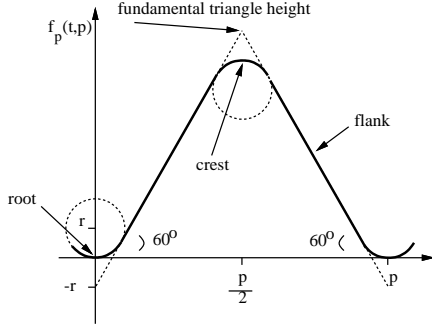
Figure 1: Thread profile.

angle before jamming. In section 4 we present an accommodation controller and in section 5 we derive conditions for jamming given the manipulator stiffness. Section 6 presents data from multiple insertions that confirms our jamming criteria.

2   Geometry

The discussion of threaded fasteners is facilitated with the introduction of some terms from [Blake 86] and [Bickford 81]. Figure 1 illustrates the most important ones.

A *screw thread* is a ridge of constant section, called the *thread profile*, wrapped in a helical fashion about a cylinder. The *pitch* is the spatial period of the thread profile. The *external screw thread* is the thread on a bolt and the *internal screw thread* is that on a nut. The *root* of the profile is at the smallest diameter and the *crest* is at the largest. The diameter used for specification of threaded parts is the largest diameter of the internal thread or the *internal thread major diameter*. The *flank* is the straight part of the thread joining the roots and the crests. If the thread were extended to a full V the *fundamental triangle height* would be reached. Instead it is rounded off or flattened at the roots and crests.

A *clearance fit* provides free-running assembly by the means of a non-zero *allowance*. Allowance is the amount by which the external thread diameter is reduced as compared to the internal thread. This paper discusses the *allowance ratio* which expresses allowance as a fraction of the internal thread major diameter.

Threads do not start immediately on a nut or bolt, but undergo a thread run-up, also called an *incomplete thread*. The form and length of the run-up plays an important role in the avoidance of *cross-threading*. Cross-threading, which leads to an incomplete and wedged assembly, occurs when the first external thread crosses the internal thread in such a way
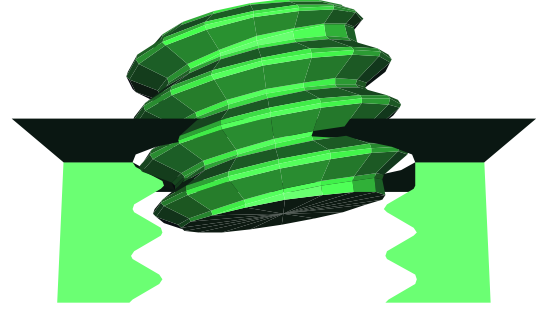

Figure 2: A cross-threaded bolt and nut configuration.

that the thread contacted on one side of the internal thread is not on the same revolution as the thread contacted on the opposite side. Figure 2 shows a bolt in a crossed thread configuration.

2.1   Functional Description

Based on the definitions given above, a rounded crest and root thread profile can be made with the following four variables.

p: pitch.

d: internal thread basic major diameter.

a: allowance ratio, $0 \leq a \leq 1$, where the actual allowance is $a * d$.

ρ: root and crest radius ratio. The root and crest radius are given by the function $r(p) = \rho p$. Typically $\rho = 0.1$.

The ratio $\frac{d}{p}$ determines if the bolt has fine or coarse threads. Typically $(\frac{d}{p})_{fine} = 2(\frac{d}{p})_{coarse}$.

The thread profile can be parameterized by the following function of position, t and thread pitch p. Figure 1 shows the function with $\rho = 0.1$. In f_p, t is understood to be $t \mod p$ and $r = r(p)$ where p is the *argument* to f_p.

$$
f_p(t, p) = \begin{cases}
r - \sqrt{r^2 - t^2} & 0 \leq t \leq \frac{\sqrt{3}}{2} r \\
\sqrt{3}\, t - r & \frac{\sqrt{3}}{2} r \leq t \leq \frac{p}{2} - \frac{\sqrt{3}}{2} r \\
\frac{\sqrt{3}}{2} p - 3r + \sqrt{r^2 - (t - \frac{p}{2})^2} & \frac{p}{2} - \frac{\sqrt{3}}{2} r \leq t \leq \frac{p}{2} + \frac{\sqrt{3}}{2} r \\
\sqrt{3}(p - t) - r & \frac{p}{2} + \frac{\sqrt{3}}{2} r \leq t \leq p - \frac{\sqrt{3}}{2} r \\
r - \sqrt{r^2 - (t - p)^2} & p - \frac{\sqrt{3}}{2} r \leq t \leq p
\end{cases}
$$

If you extend the thread profile for an integral number of threads and align the t-axis with the z-axis in a right hand coordinate system, a screw thread can be created by rotating the profile about the z-axis at a radius $\frac{d}{2}$ and vertically shifting at the same time. The vertical shift is $p(\frac{\theta}{2\pi})$ where θ is the amount of rotation.
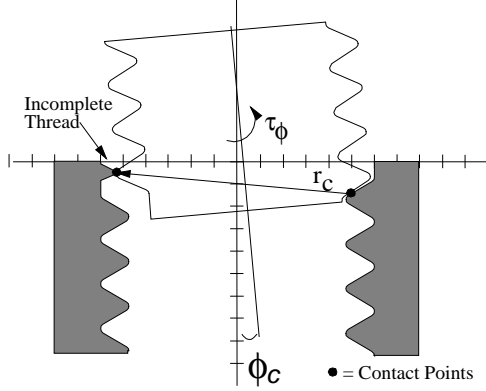
Figure 3: Cross thread tilt angle

A surface in $\Re^3$ may be parameterized by 2 variables. The parameters z and θ have been chosen. Thus a point on the surface of the nut is given by the cylindrical coordinates: $(r_{int}(z,\theta),\theta,z)$. Similarly a point on the surface of the bolt is given by: $(r_{ext}(z,\theta),\theta,z)$. r_{ext} and r_{int} represent the external thread radius and internal thread radius respectively. For $z < 0$, r_{ext} is undefined. Similarly r_{int} is undefined for $z > 0$. The image in Figure 2 was created using these functions. (In the figure $\frac{d}{p} = 6.0, \rho = 0.1, a = 0.05$.) r_{int} and r_{ext} include a linear thread run-up over 180 degrees.

$$r_{int}(z,\theta) = \begin{cases} \frac{d}{2} - f_p(-z, p\frac{\pi-\theta}{\pi}) & \begin{cases} 0 \le \theta \le \pi \\ z \ge -p\frac{\pi-\theta}{\pi} \end{cases} \\ \frac{d}{2} - f_p(p - (z + p\frac{2\pi-\theta}{2\pi}), p) & z \le -p\frac{2\pi-\theta}{2\pi} \\ \frac{d}{2} & \text{otherwise} \end{cases}$$

$$r_{ext}(z,\theta) = \begin{cases} \frac{d}{2}(1-a) - (p\frac{\sqrt{3}}{2} - 2r) + & \begin{cases} \pi \le \theta \le 2\pi \\ f_p(z, p\frac{\theta-\pi}{\pi}) & z \le p\frac{\theta-\pi}{\pi} \end{cases} \\ \frac{d}{2}(1-a) - (p\frac{\sqrt{3}}{2} - 2r) + & \\ f_p(z - p\frac{\theta}{2\pi}, p) & z \ge p\frac{\theta}{2\pi} \\ \frac{d}{2}(1-a) - (p\frac{\sqrt{3}}{2} - 2r) & \text{otherwise} \end{cases}$$

$$(1)$$

3 Maximum Tilt Angle

During the insertion of threaded fasteners the maximum angle of tilt decreases as the insertion progresses. To avoid cross threading during the initial insertion phase the first full external thread must not be allowed to cross under the crest of the *incomplete* internal thread. We can determine the smallest angle at which this can occur by considering the two point contact configuration shown in Figure 3. One contact is between the crest of the first complete external thread and the crest of the incomplete internal thread. The other contact is at the junction of the root and flank
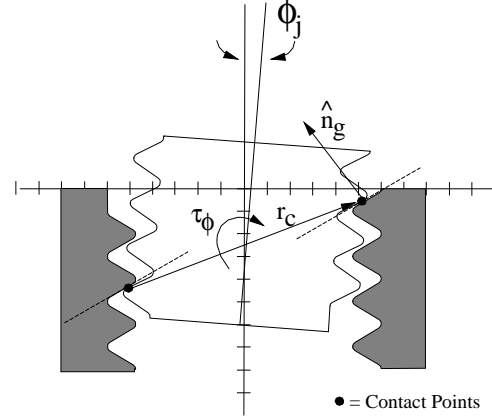

Figure 4: Jamming tilt angle

of the external and internal thread. $\mathbf{r}_c$ is the vector between the contact points. In the worst case of $a = 0$ the cross thread angle, ϕ_c, is given as:

$$\begin{aligned} \phi_c &= \arctan(\frac{p}{2}, |\mathbf{r}_c|) \\ &> \frac{p}{2(1-a)d} \end{aligned} \qquad (2)$$

where $\mathbf{r}_c$ is the vector between the contact points as shown in the figure. The inequality comes from the fact that $\rho < \sqrt{3}/8$. Note that this angle is $1/2$ that given by [Nevins and Whitney 89] as we consider the cross threading angle to be the *minimum* tilt angle for the onset of cross threading.

For situations when the bolt has been inserted so that fully formed threads are mating, the maximum possible tilt will be given by the angle ϕ_j. ϕ_j may be determined by determining the translation and rotation of the bolt necessary for the points on the bolt shown in Figure 4 to lie on the lines given by the flanks of the nut. Using small angle approximations we derive:

$$\phi_j(\lambda) = \frac{a}{2\sqrt{3}\left(\frac{1}{2}(1-a) - \frac{p}{d}\left(\rho - \frac{\lambda - \frac{1}{2}}{2\sqrt{3}}\right)\right)} \qquad (3)$$

where λ is the depth of insertion in number of threads. As would be expected, ϕ_j increases quickly with the allowance ratio a.

Given standard bolt dimensions ϕ_c is typically 3 or 4 times larger than $\phi_j(1)$. This indicates, as [Nevins and Whitney 89] point out, that for all but the smallest fasteners ϕ_c is large enough to avoid cross threading. However, if the manipulator controlling the insertion is stiff in the tilt direction (as it would have
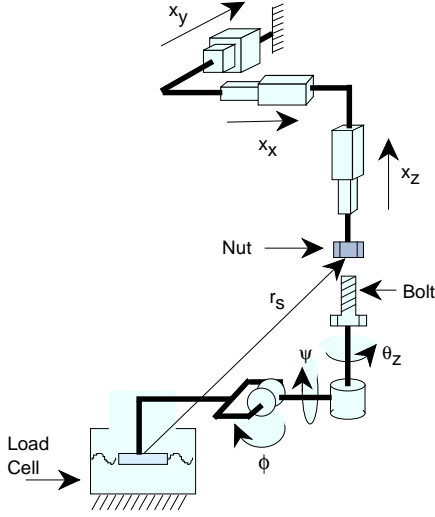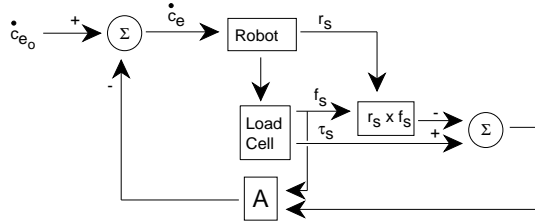
Figure 5: Manipulator kinematics.

Figure 6: Controller structure.

have to be to ensure angular errors less than a few tenths of a degree), then it may jam if the initial tilt is greater than $\phi_j(1)$. This is explained further in the following sections.

4 Control

If we assume the nut to be fixed in space, then the configuration of the bolt with respect to the nut can be described by a 6 dimensional configuration vector $\mathbf{c}$:

$$\mathbf{c} = \left[\begin{array}{cc} \mathbf{x} & \boldsymbol{\theta} \end{array} \right]^T$$

where $\mathbf{x} \in \Re^3$ and $\boldsymbol{\theta} \in SO(3)$, the rotation space. The global origin is located at the center of the top of the nut. The origin of the body, or bolt, frame is at the center of the base of the bolt. The components of $\boldsymbol{\theta}$ and $\mathbf{x}$, illustrated in Figure 5, will be referred to as:

$$\boldsymbol{\theta} = \left[\begin{array}{ccc} \phi & \psi & \theta_z \end{array} \right] \quad , \quad \mathbf{x} = \left[\begin{array}{ccc} x_x & x_y & x_z \end{array} \right] \ .$$

Using a linear model for the combined structural and servo stiffness of the manipulator we have a force

and torque which are a function of the displacement from the equilibrium or set-point configuration $\mathbf{c}_e$. We denote the force due to the compliance of the manipulator in the inertial frame by $\mathbf{f}_a$. The inertial torque applied by the controller about the origin of the nut is denoted by $\boldsymbol{\tau}_a$. If we assume quasistatics, the total force and torque on the bolt due to contact with the nut is given by:

$$\left[\begin{array}{c} \mathbf{f}_a(\mathbf{c}, \mathbf{c}_e) \\ \boldsymbol{\tau}_a(\mathbf{c}, \mathbf{c}_e) \end{array} \right] = \mathbf{K}(\mathbf{c}_e - \mathbf{c}) \qquad (4)$$

where $\mathbf{K}$ is the stiffness of the manipulator.

In the presence of low sensor noise and low uncertainty in the relative position between the sensor origin and the origin of the bolt held by the manipulator, $\boldsymbol{\tau}_a$ and $\mathbf{f}_a$ can be estimated with:

$$\left[\begin{array}{c} \hat{\mathbf{f}}_a \\ \hat{\boldsymbol{\tau}}_a \end{array} \right] = \left[\begin{array}{c} \mathbf{f}_s \\ \boldsymbol{\tau}_s - \mathbf{r}_s \times \mathbf{f}_s \end{array} \right]$$

where $\mathbf{f}_s$ and $\boldsymbol{\tau}_s$ are the sensed force and torque at the sensor origin and $\mathbf{r}_s$ is the vector from the sensor origin to the bolt origin.

Assuming that the manipulator allows velocity control and is fitted with a force sensing device, we can use an accommodation matrix [Schimmels 90] to servo the velocity based on the force feedback according to:

$$\dot{\mathbf{c}}_e = \dot{\mathbf{c}}_{e_o} - \mathbf{A} \left[\begin{array}{c} \hat{\mathbf{f}}_a \\ \hat{\boldsymbol{\tau}}_a \end{array} \right] \qquad (5)$$

Figure 6 illustrates the controller structure.

The choice of non-zero elements in $\mathbf{A}$ is based on our assumptions about initial positioning uncertainty. Since we typically will want the fastest response possible, the magnitudes will be chosen to be the largest that ensure stability of the controller based on the servo rate.

5 Accommodation and jamming

We start by noting that errors in $\mathbf{x}$ may be easily corrected as nuts typically have large chamfers. Thus, as the analyses of [Nevins 80] and [Schimmels 90] show, either low stiffness or high accommodation will correct for these types of errors. Our main concern becomes the control of the tilt angle and the avoidance of cross-threading and jamming.

To guarantee proper assembly of the threaded fasteners with a simple linear controller, the initial value for $\phi = \phi_o$ must be less than ϕ_c during the initial insertion phase. This can be seen from figures 3 and 4,

as an error of $\phi_j(1) < \phi_o < \phi_c$ will result in a correcting torque τ_ϕ, but an error of $\phi_o > \phi_c$ will result in a τ_ϕ that will increase ϕ.

If we know $\phi_o < \phi_c$ than we can use a controller with a high tilt stiffness to ensure that it does not tilt beyond ϕ_c during the assembly. In doing this, however, we must avoid jamming that may occur if $\phi_o > \phi_j(1)$.

To derive the jamming condition we first assume that due to either low stiffness or high accommodation $\mathbf{f}_a$ is small. Jamming for $\phi_o < \phi_c$ will be due to a two point contact as illustrated in Figure 4. The condition for jamming is:

$$f_t < \mu f_n$$

where f_t and f_n are the magnitudes of the tangential and normal forces. At each contact, then, $\mathbf{f}_{c_i}$ is:

$$\mathbf{f}_{c_i} = f_{n_i}\hat{\mathbf{n}}_{g_i} + f_{t_i}\hat{\mathbf{v}}_{c_i}$$

The surface normal at the contact points can be found from equation (1) and the direction of sliding will be:

$$\mathbf{v}_c = \dot{\mathbf{x}} + \dot{\mathbf{R}}(\boldsymbol{\theta})\mathbf{x}_b$$

where $\mathbf{x}_b$ is the location of the contact point in the bolt frame. If we neglect the helix angle and assume the contacts to be on the nut flank at $\theta = 0$ and $\theta = \pi$ with the depth of insertion $\lambda = 1$, we can simplify this considerably using:

$$\hat{\mathbf{n}}_g \simeq \begin{bmatrix} -\frac{1}{2} \\ 0 \\ \frac{\sqrt{3}}{2} \end{bmatrix}, \mathbf{r}_c \simeq \begin{bmatrix} (1-a)d - r \\ 0 \\ \frac{p}{2} + \sqrt{3}r \end{bmatrix}, \hat{\mathbf{v}}_c \simeq \begin{bmatrix} 0 \\ -1 \\ 0 \end{bmatrix}$$

where $\hat{\mathbf{n}}_g$ is the normal at one contact and the negative of the normal at the other, $\mathbf{r}_c$ is the vector between the contact points, and $\hat{\mathbf{v}}_c$ is the direction of sliding. Under the assumption $\mathbf{f}_a = 0$ the contact forces and moment arms are equal and opposite and:

$$\mathbf{r}_c \times \mathbf{f}_c = \boldsymbol{\tau}_z + \boldsymbol{\tau}_\phi + \boldsymbol{\tau}_\psi$$

We can now derive the condition for jamming as:

$$\begin{aligned} \tau_z &< \frac{2((1-a)d - r)\mu}{\frac{p}{2} + \sqrt{3}r + \sqrt{3}((1-a)d - r)}\tau_\phi \\ &< \frac{2}{\sqrt{3}}\mu\tau_\phi \end{aligned} \quad (6)$$

Recalling our stiffness formulation for the manipulator let:

$$\tau_\phi = K_\phi(\phi_o - \phi_j(\lambda))$$

If we assume the controller can assert a maximum τ_z of τ_m then we can see why a simple linear stiffness will **not** help for situations in which $\phi_j(1) < \phi_o < \phi_c$. For jamming to be avoided we must have:

$$K_\phi < \begin{cases} \frac{2\mu\tau_m}{\sqrt{3}(\phi_o - \phi_j(\lambda))} & \phi_o > \phi_j(\lambda) \\ \infty & \phi_o < \phi_j(\lambda) \end{cases} \quad (7)$$

for λ as large as the depth of insertion, often as large as 10. For most practical situations this will yield either a controller too compliant to avoid cross threading or a controller with a large maximum torque.

An alternative would be to maintain a large K_ϕ until $\lambda = 1$ and then decrease it as the danger of cross threading will be passed. Identification of this situation is of key importance for future research.

6   Experiments

Given the previous results, we constructed the apparatus shown schematically in Figure 5 to corroborate them. A two degree of freedom Sawyer motor in combination with 2 dc servo motors, a rotary stepper motor and a six axis load cell controlled the position, velocity, and stiffness of the bolt. The force sensor was accurate to 0.1 N and 0.3 Ncm. The RobotWorld module can be positioned with an accuracy of 0.0005 cm. The dc motors controlled servo compliance in the x_z and θ_z directions. A 1KHz loop tracked the set velocities from a 25Hz loop that read from the force torque sensor. The manipulator can be described by the following stiffnesses:

$$\begin{aligned} \mathbf{K} &= \operatorname{diag}\begin{bmatrix} \mathbf{K}_x & \mathbf{K}_\theta \end{bmatrix} \\ \mathbf{K}_x &= \begin{bmatrix} 170 & 170 & 70 \end{bmatrix}\frac{\text{N}}{\text{cm}} \\ \mathbf{K}_\theta &= \begin{bmatrix} 50 & 50 & 2.6 \end{bmatrix}\frac{\text{N cm}}{\text{degree}} \end{aligned}$$

During insertion the nominal trajectory was:

$$\dot{\mathbf{c}}_{e_o} = \begin{bmatrix} 0 & 0 & -0.0238\frac{\text{cm}}{\text{s}} & 0 & 0 & -57.3^o\frac{1}{\text{s}} \end{bmatrix}^T$$

To correct for errors in $\mathbf{x}$ the following accommodation matrix was used:

$$\mathbf{A} = \operatorname{diag}\begin{bmatrix} 0.03 & 0.03 & 0.0 & 0.0 & 0.0 & 0.0 \end{bmatrix}\frac{\text{cm}}{\text{s} \cdot \text{N}}$$

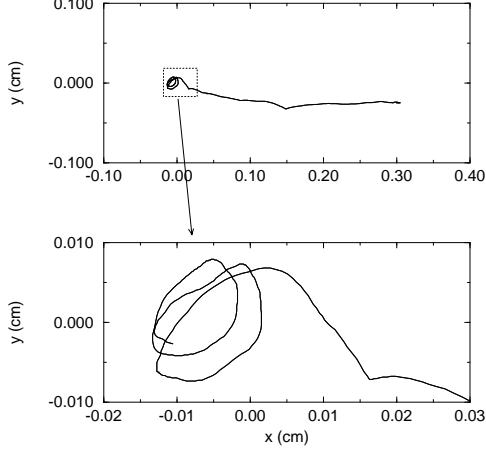| p	d	a	$\phi_j(1)$	ϕ_c
0.14 cm	1.46 cm	0.024	0.8^o	2.8^o

Table 1: Bolt parameters.

Figure 7: XY Trajectory during assembly, whole and magnified parts

The magnitude of the accommodation was the largest possible that would not be unstable at the 25Hz update rate. Table 1 shows the bolt parameters and predicted tilt angles for the bolt used in the experiments.

In reviewing the experiments we first review data from single trials and then we will review data from all the trials. Figure 7 shows that the simple accommodation controller could easily correct for errors in **x**. The top plot shows the path from the initial offset in x_x of 0.3 cm and the enlarged plot shows an interesting spiralling motion that occurs once the bolt is inserted by more than one thread. In this case the tilt angle was kept small to ensure proper insertion with:

$$\mathbf{c}_e(0) = \begin{bmatrix} 0.3\text{cm} & 0.0 & 0.0 & 0.2^\circ & 0.0 & 0.0 \end{bmatrix}^T$$

Figure 8 shows how the fastening signature, or plot of τ_z versus θ_z varies with ϕ. For ϕ near ϕ_c, τ_z increases sharply with θ_z, whereas for a smaller tilt the increase is more gradual.

Figure 9 confirms the effective friction angle presented in equation (6). If we take $\mu = 0.18$, which is typical for a steel/steel contact [Oberg 46], then equation (6) predicts τ_z/τ_ϕ of 0.21, which compares favorably with the data.

The most interesting results come from checking the validity of the tilt angle equation (3) and the stiffness condition equation (7). To do this we ran 110 insertions varying the initial configurations with:
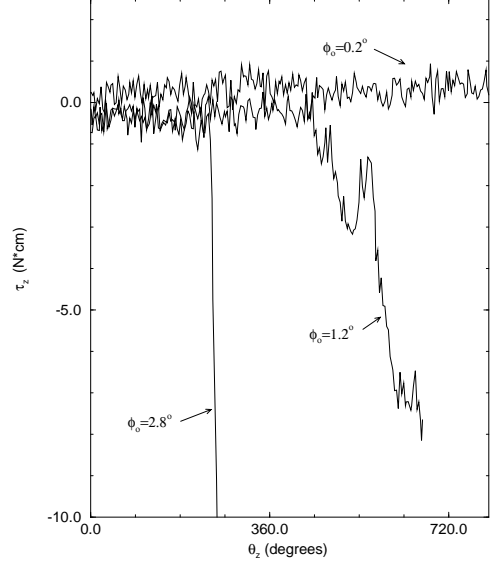

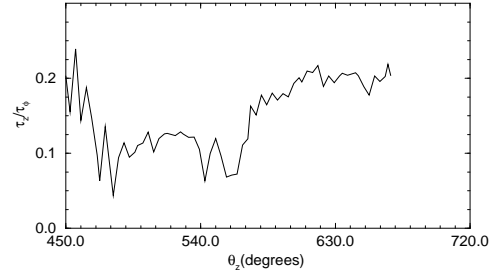Figure 8: Fastening signature for different tilt angles

Figure 9: Effective friction when $\phi_o = 1.2$.

$$x_z = 0.42\text{cm}$$
$$-0.3 < x_x < 0.3, \qquad -0.3 < x_y < 0.3$$
$$-1080 < \theta_z < -720, \qquad 0 < \phi_o < 2.5$$

The insertions terminated if either $\tau_z < -8.0$Ncm or if $z < -2.2p$. Figure 10 plots the trials showing the number of engaged threads before termination for different values of ϕ_o. Also plotted is the inverse of equation (3):

$$\lambda_j(\phi, a) = \frac{1}{2} + 2\sqrt{3}\rho - \frac{d}{p}((1-a)\sqrt{3} + \frac{a}{\phi}) \quad (8)$$

As you can see the line for $a = .024$ does not fit the data as well as for $a = .035$. The value of $a = 0.024$ was determined by measuring the amount of translation freedom for the nut once inserted. Figure 7 shows this may be even a generous estimate. An offset of a tenth of a degree of our apparatus would also explain this difference. We were encouraged that the slope of the data, though very steep, does match equation (8).
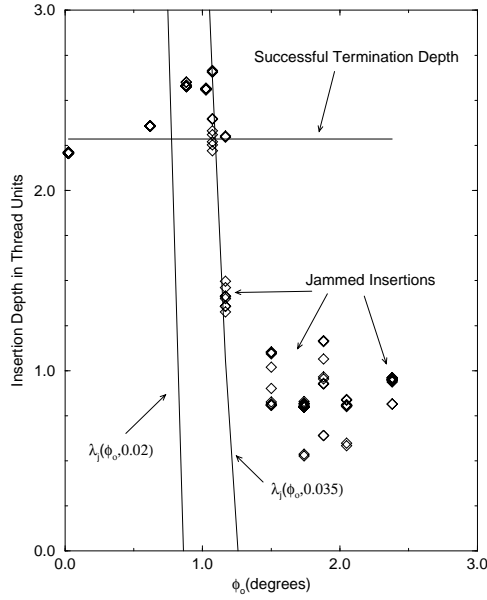
Figure 10: Number of threads engaged at termination

7   Conclusions

We have presented a model for compliant insertion of threaded parts and compared that model to experimental data. It is clear that control of the tilt angle is essential to ensure proper mating. It is also clear that a simple linear controller will not work due to the confusion between torques about the tilt direction due to a jam and those due to cross threading. The slope of the fastening signature does give some indication of the degree of tilt, however it is not a clear enough indicator by itself to determine the tilt angle. Future research should focus on methods to determine the tilt angle from force information.

8   Acknowledgements

We thank Matthew Mason for providing the reference to [Blaer 62].

References

[Bickford 81] J.H. Bickford, *An Introduction to the Design and Behavior of Bolted Joints,* Marcel Dekker, Inc., New York, 1981.

[Blaer 62] I.L. Blaer, "Reliable Starting of Threads," *Russian Engineering Journal,* v.42, n. 12, 1962.

[Blake 86] A. Blake, *Threaded Fasteners,* Marcel Dekker Inc., New York, 1986.

[Lozano-Perez 84] T. Lozano-Perez, M.T. Mason and R.H. Taylor, "Automatic Synthesis of Fine-Motion Strategies for Robots," *The Int. Journal of Robotics Research,* Vol. 3, No. 1, Spring 1984.

[Mikels 91] M.E. Mikels, Marshall Builders, Inc. 115 15th Ave., San Mateo, CA, Patent Pending.

[Nevins 80] J.L. Nevins and D.E. Whitney, "Assembly Research," *Factory Automation* v. 2, 1980, Maidenhead, England.

[Nevins and Whitney 89] J.L. Nevins and D.E. Whitney ed., *Concurrent Design of Products and Processes,* New York, McGraw-Hill, 1989.

[Nicolson 90] E.J. Nicolson, "Grasp Stiffness Solutions for Threaded Insertion," U.C. Berkeley M.S. Thesis, December 1990.

[Nicolson and Fearing 91] E.J. Nicolson and R.S. Fearing, "Dynamic Simulation of a Part Mating Problem: Threaded Fastener Insertion," *Int. Conf. on Intelligent Robots and Systems (IROS),* Osaka Japan, November 1991.

[Oberg 46] E. Oberg and F.D. Jones, *Machinery's Handbook,* The Industrial Press, Machinery Publishing Co., 1946

[Schimmels 90] J.M. Schimmels and M.A. Peshkin, "Synthesis and Validation of Non-Diagonal Accommodation Matrices for Error-Corrective Assembly," *Proc. 1990 IEEE Conf. on Robotics and Automation,* Cincinnati, OH, May 1990.

[Smith 80] S.K. Smith, "Use of a Microprocessor in the control and Monitoring of Air Tools while Tightening Threaded Fasteners," Eaton Corporation, *Autofact West,* Proc. Vol. 2, Society of Manufacturing Engineers, Dearborn, MI, 1980.

[Strip 88] D.R. Strip, "Insertions Using Geometric Analysis and Hybrid Force-Position Control: Method and Analysis," *Proc. 1988 IEEE Int. Conf. on Robotics and Automation,* Philadelphia, PA April 1988.

[Tao 90] J.M. Tao, J.Y.S. Luh and Y.F. Zheng, "Compliant Coordination Control of Two Moving Industrial Robots," *IEEE Trans. on Robotics and Automation* Vol. 6, No. 3, June 1990.

[Tsujimura 91] T. Tsujimura and T. Yabuta, "Adaptive force control of screwdriving with a positioning-controlled manipulator," Robotics and Autonomous Systems,Vol 7, no. 1, March 1991, 57-65.

[Weber] Weber Screwdriver Systems, Inc., 45 Kensico Drive, Mount Kisco, New York.

[Whitney 82] D.E. Whitney, "Quasi-Static Assembly of Compliantly Supported Rigid Parts," *Jnl. of Dynamic Systems, Measurement, and Control,* March 1982, Vol. 104.